Supporting Information

Scanning the Optoelectronic Properties of $Cs_4Cu_xAg_{2-2x}Sb_2Cl_{12}$ Double Perovskite Nanocrystals: Role of Cu^{2+} Content

Ye Zhang[a], Ning Sui[a,], Zhihui Kang[a], Xiangdong Meng[c], Long Yuan[c], Xianfeng Li[a] and Han-zhuang Zhang[a], Jiaqi Zhang[b,*] and Yinghui Wang[a,*]*

[a] *Femtosecond Laser laboratory, Femtosecond Laser laboratory, Key Laboratory of Physics and Technology for Advanced Batteries, College of Physics, Jilin University, Changchun 130012, P. R. China.*

E-mail: yinghui_wang@jlu.edu.cn, sui@jlu.edu.cn

[b] *Key Laboratory of Automobile Materials, Ministry of Education, College of Materials Science and Engineering, Jilin University, Changchun 130012, China.*

E-mail: zhangjiaqi@jlu.edu.cn.

[c] *Key Laboratory of Functional Materials Physics and Chemistry of the Ministry of Education, Jilin Normal University, Changchun, P. R. China;*

† These authors contributed equally to this work

Section 1. Calculation Details of nonlinear absorption coefficient (β) and the two-photon absorption cross section (σ)

The influence of the solvent nonlinearity could be excluded. The two-photon absorption (TPA) coefficient β of $Cs_4Cu_xAg_{2-2x}Sb_2Cl_{12}$ in toluene solvents can be obtained by fitting the experimental results with equation:[1-3]

$$T(z,S=1)=\sum_{m=0}^{\infty}\frac{\left[-q_0(z,0)\right]^m}{(m+1)^{3/2}}$$

where $q_0(z)=\beta I_0/(1+z^2/z_0^2)$; $z_0=k\omega_0^2/2$ is the Rayleigh length, $k=2\pi/\lambda$ is the wave vector, ω_0 is beam waist radius of Gaussian pulse, and I_0 is the pulse irradiance. The TPA coefficient β is related to the TPA cross section σ by using[4]

$$\sigma=\frac{\beta h\upsilon 10^3}{Nc}$$

where *N* is Avogadro's number, *c* is the concentration, *h* is Planck's constant, and *v* is the laser frequency. In this experiment, the concentration of $Cs_4Cu_xAg_{2-2x}Sb_2Cl_{12}$ is 2.0×10^{-5} (*x* = 0.60), 1.6×10^{-5} (*x* = 0.75), 1.8×10^{-5} (*x* = 0.90) and 1.9×10^{-5} (*x* = 1.00) M, respectively. σ is expressed in Göppert-Mayer units (GM), with 1 GM = 1×10^{-50} cm^4 s $molecule^{-1}$ $photon^{-1}$.

Section 2: Calculation of average numbers of absorbed photons <N>, absorption cross-section σ

The probability of a nanocrystal contains N excitons is described by Poisson distribution (Eq. S1):

$$P_N=\frac{e^{-\langle N\rangle}\times\langle N\rangle^N}{N!} \quad \text{(S1)}$$

where ⟨N⟩ is the average number of photons per nanocrystal and can be calculated by (Eq. S2):

$$\langle N\rangle=j\sigma \quad \text{(S2)}$$

where σ is the absorption cross section, and j is incident photon density per pulse. We can calculate σ by (Eq. S3)

$$P_{max}=\sum_{N=1}^{\infty}P_N=1-P_0=1-e^{-\langle N\rangle}=1-e^{-j\sigma} \quad \text{(S3)}$$

σ of NCs can be obtained by fitting the data with equation of $1-e^{-j\sigma}$ (solid line in Fig. 3b).

Section 3. Table and Figure

Table S1. Fitting results for the XPS patterns of elements composition ratios for $Cs_4Cu_xAg_{2-2x}Sb_2Cl_{12}$ perovskite NCs.

At. %	**X = 0.60**	**X = 0.75**	**X = 0.90**	**X = 1.00**
Cs	21.25	22.14	20.89	18.8
Cu	2.16	3.20	4.18	5.00
Ag	2.89	2.01	0.93	0.00
Sb	12.06	11.25	11.09	11.20
Cl	61.20	60.89	62.70	63.50

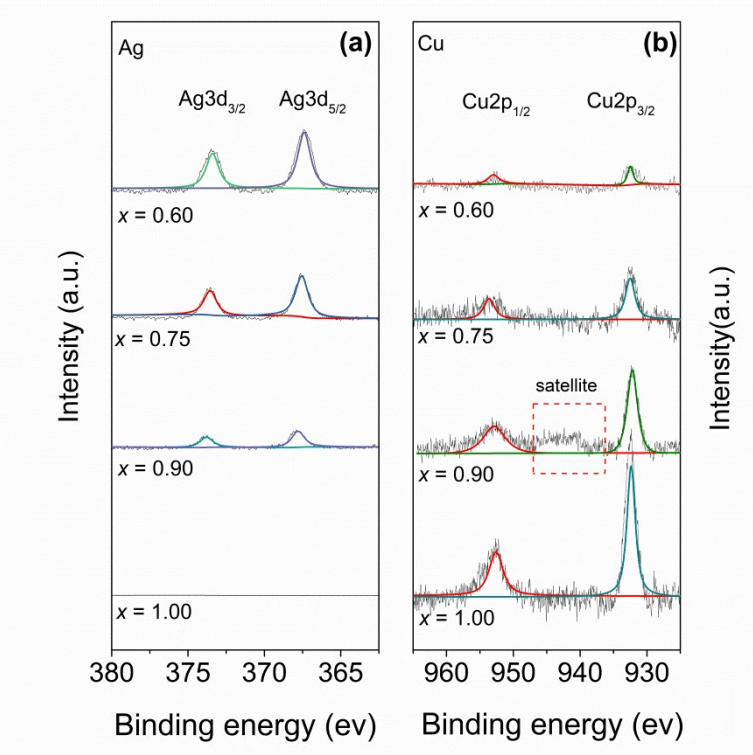

Fig. S1. XPS spectra of $Cs_4Cu_xAg_{2-2x}Sb_2Cl_{12}$ (x = 0.60, 0.75, 0.90 and 1.00) samples for (a) Ag 3d and (b) Cu 2p signals, which is consistent with the previous report[5]. The spectra have calibrated using the Carbon 1s peak. The red square shows that the satellite peaks are located between 940 eV and 950 eV (x = 0.90), suggesting that the Cu^{2+} really exists in our samples[6].

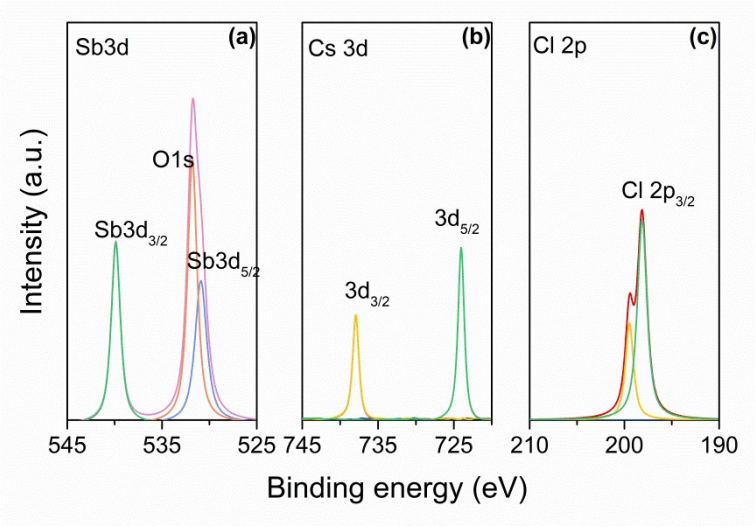

Fig. S2. The fitting XPS spectra for Cs 3d, Cl 2p and Sb 3d signals of $Cs_4CuSb_2Cl_{12}$ NCs. The spectra have been calibrated using the Carbon 1s peak.

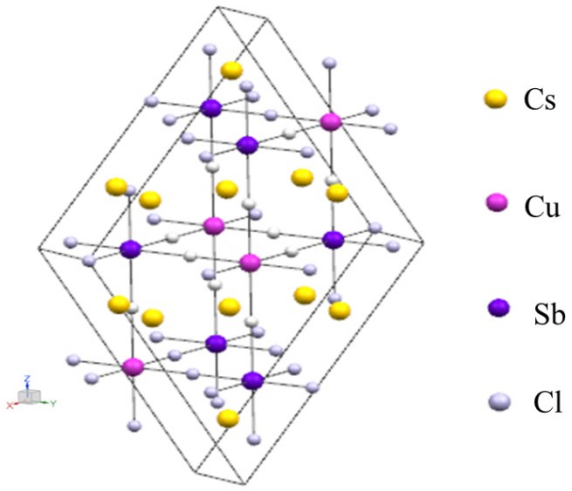

Fig. S3. Scheme of the atomic models for the $Cs_4CuSb_2Cl_{12}$ layered double perovskite.

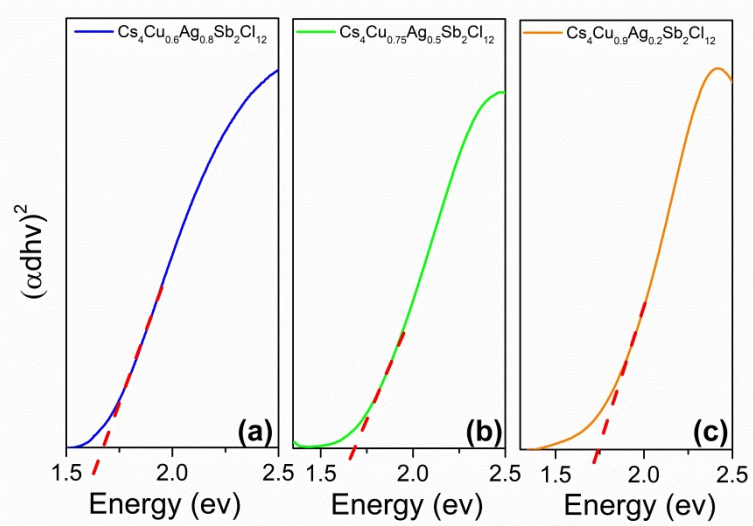

Fig. S4. Bandgaps of $Cs_4Cu_xAg_{2-2x}Sb_2Cl_{12}$ perovskite NCs (x = 0.60 (a), 0.75 (b), 0.90 (c) from left to right) estimated by Tauc plot. Bandgap is extrapolated from the linear portion of the $(\alpha dhv)^2$ versus the hv curve in the direct band gap Tauc plots, where α is the absorption coefficient, d is the sample thickness, and hv is the photon energy.

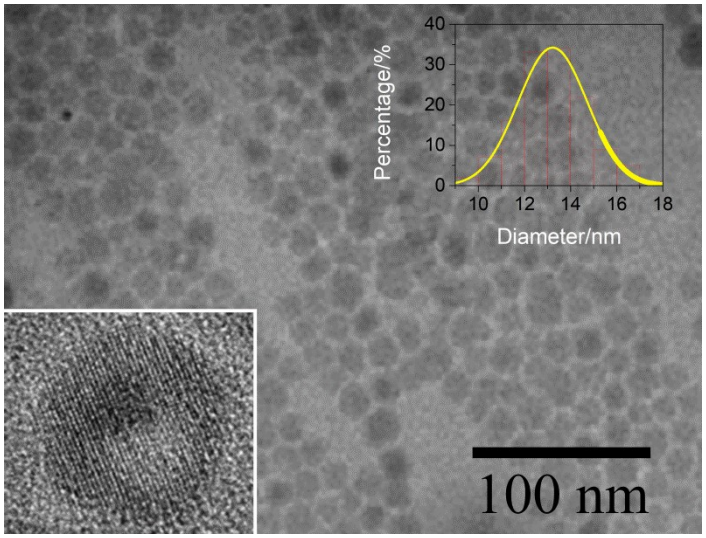

Fig. S5. TEM image of $Cs_4Cu_xAg_{2-2x}Sb_2Cl_{12}$ perovskite NCs (x = 0.60). Inset: HR-TEM imaging and size distribution image.

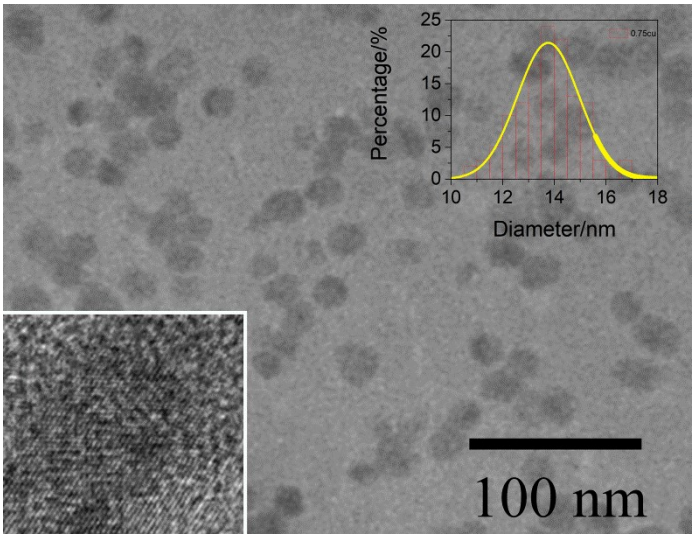

Fig. S6. TEM image of $Cs_4Cu_xAg_{2-2x}Sb_2Cl_{12}$ perovskite NCs (x = 0.75). Inset: HR-TEM imaging and size distribution image.

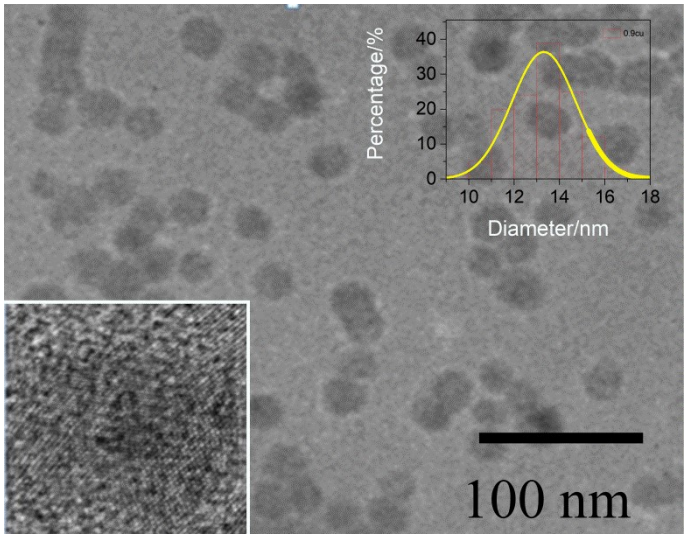

Fig. S7. TEM image of $Cs_4Cu_xAg_{2-2x}Sb_2Cl_{12}$ perovskite NCs (x = 0.90). Inset: HR-TEM imaging and size distribution image.

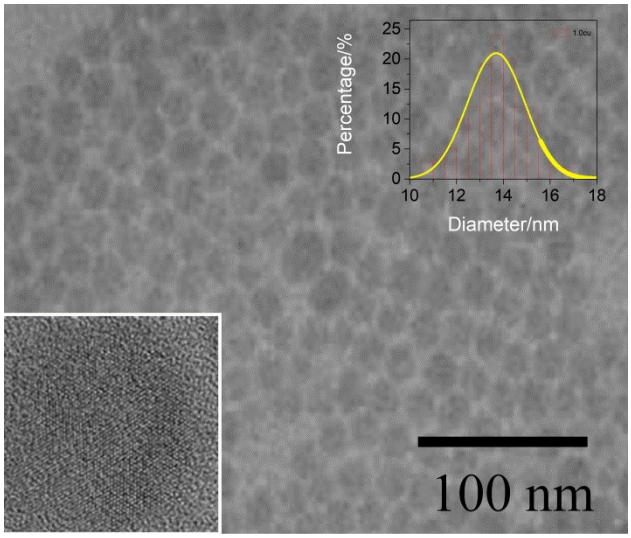

Fig. S8. TEM image of $Cs_4Cu_xAg_{2-2x}Sb_2Cl_{12}$ perovskite NCs (x = 1.00). Inset: HR-TEM imaging and size distribution image.

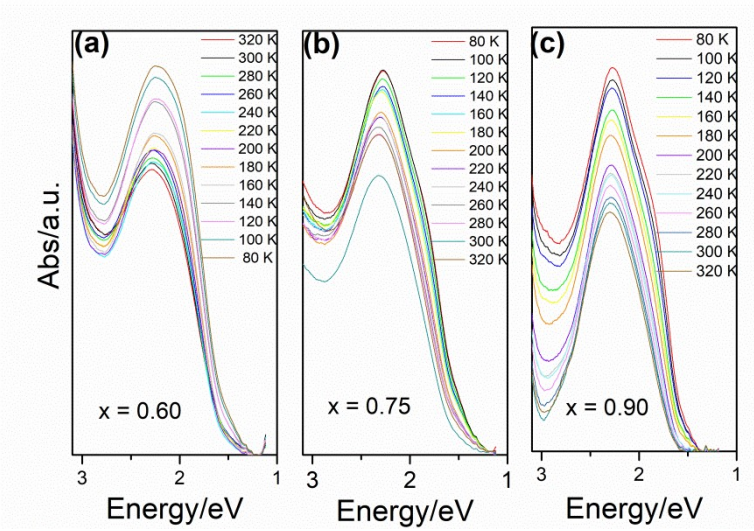

Fig. S9. Temperature-dependent absorption spectra of $Cs_4Cu_xAg_{2-2x}Sb_2Cl_{12}$ perovskite NCs (x = 0.60 (a), 0.75 (b), 0.90 (c) from left to right).

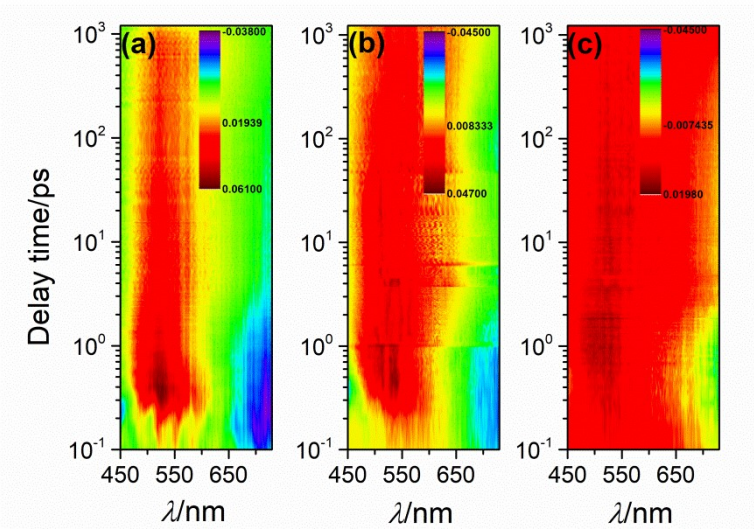

Fig. S10. Contour plot of the TA data of $Cs_4Cu_xAg_{2-2x}Sb_2Cl_{12}$ perovskite NCs (x = 0.90 (a), 0.75 (b) and 0.60 (c) from left to right).

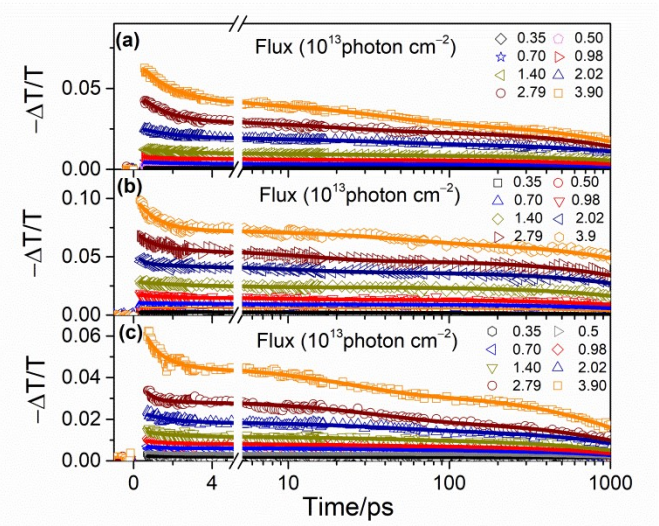

Fig. S11. Bleach kinetics of $Cs_4Cu_xAg_{2-2x}Sb_2Cl_{12}$ perovskite NCs (x = 0.90 (a), 0.75 (b), 0.60 (c) from top to bottom) under various flux, in which the solid lines are the fits to the kinetic traces according to the carrier recombination model.

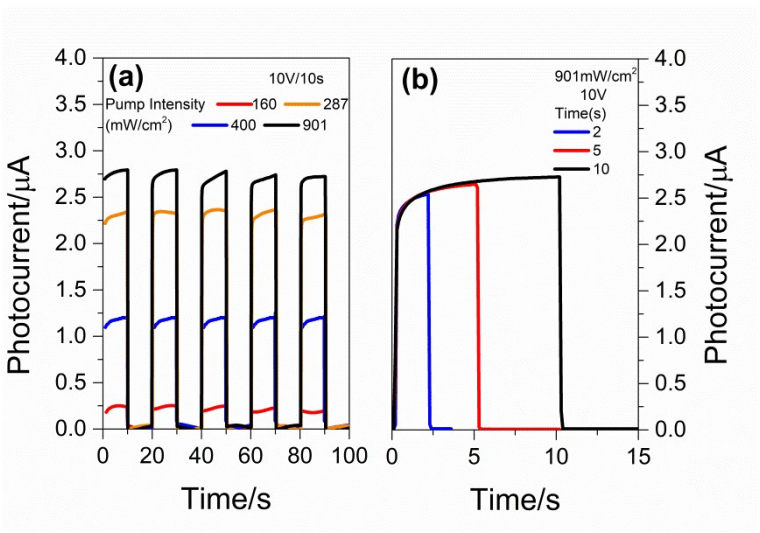

Fig. S12. Response-current of photodetector based on $Cs_4Cu_{0.60}Ag_{0.80}Sb_2Cl_{12}$ NC as a function of pump intensities (a) and time (b).

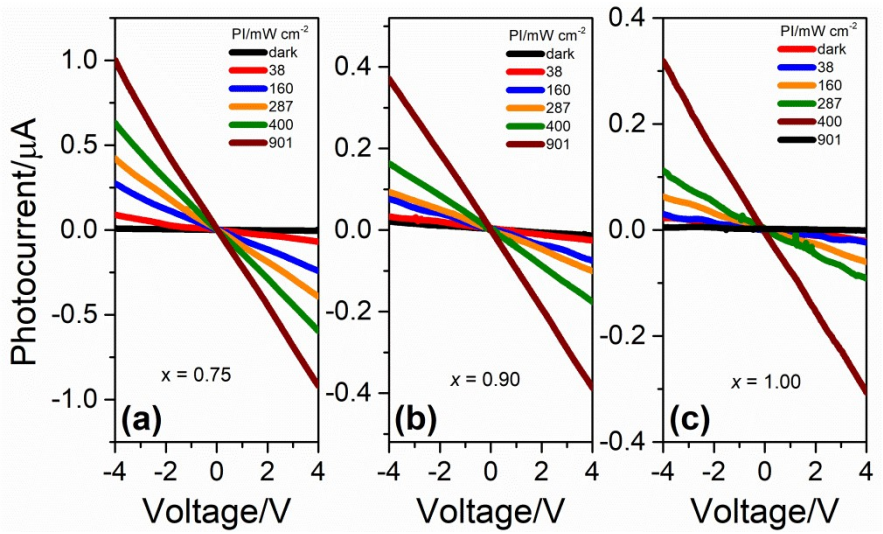

Fig. S13. I-V curve for varying intensities of $Cs_4Cu_xAg_{2-2x}Sb_2Cl_{12}$ perovskite NCs (x = 1.00 (c), 0.90 (b), 0.75 (a) from right to left)

References:

1. Huang, T.-H., et al., *Opt. Mater.* 2013, ***35***, 467-471.
2. Sheik-Bahae, M.; Said, A. A., *IEEE J. Quantum Electron.* 1990, ***26***, 760-769.
3. Zhang, Y.; Wang, Q.; Sui, N.; Kang, Z.; Li, X.; Zhang, H.-z.; Zhang, J.; Wang, Y., *Appl. Phys. Lett.* 2021, ***119***.
4. Ho-Wu, R.; Yau, S. H.; Goodson, T., *ACS Nano* 2016, ***10***, 562-572.
5. Cai, T., et al., *J. Am. Chem. Soc.* 2020, ***142***, 11927-11936.
6. P. P, A.; Joshi, M.; Verma, D.; Jadhav, S.; Choudhury, A. R.; Jana, D., *ACS Applied Nano Materials* 2021, ***4***, 1305-1313.